IEEE Access
Multidisciplinary | Rapid Review | Open Access Journal

Received June 17, 2020, accepted July 6, 2020, date of current version July 28, 2020.

Digital Object Identifier 10.1109/ACCESS.2020.3008776

Low-Loss Low-Back-Reflection Coupling of Hollow-Core Photonic Bandgap Fiber With Integrated-Optic Circuit in Fiber Optic Gyroscope

NINGFANG SONG, CHENG HE, XIAOBIN XU, JIAQI LIU, FUYU GAO, AND YUNHAO ZHU
School of Instrument Science and Opto-Electronics Engineering, Beihang University, Beijing 100191, China

Corresponding author: Xiaobin Xu (xuxiaobin@buaa.edu.cn)

This work was supported in part by the National Natural Science Foundation of China under Grant 61935002.

ABSTRACT Photonic bandgap fiber-optic gyroscope has excellent environment adaptability and shows great prospect. The coupling between hollow-core photonic bandgap fiber coil and integrated-optic circuit is a crucial technology in photonic bandgap fiber-optic gyroscope. A low-loss low-back-reflection method for the coupling between a hollow-core photonic bandgap fiber and integrated-optic circuit is proposed. The end-face of the hollow-core photonic bandgap fiber only needs to be flat-cleaved with a general fiber cleaver. The optimal coupling angle is determined and experimentally verified to overcome the effect caused by the air gap between angle-cleaved integrated-optic circuit and flat-cleaved hollow-core photonic bandgap fiber end-face. Experimental results reveal that the coupling loss and back-reflection of the hollow-core photonic bandgap fiber with the integrated-optic circuit are better than ∼3.2 dB and ∼−43 dB, respectively. Compared with conventional butt coupling and fusion splicing, the coupling performance of the proposed method is significantly improved, which can achieve low-loss, low-back-reflection, and high reliability. The method provides a foundation for the coupling between hollow-core photonic bandgap fiber coil and integrated-optic circuit in fiber optic gyroscope.

INDEX TERMS Gyroscopes, hollow-core photonic bandgap fibers, integrated-optic circuit, optical fiber sensors.

I. INTRODUCTION

The fiber optic gyroscope (FOG) is an optical fiber rotation sensor based on Sagnac effect [1]. Hollow-core photonic bandgap fibers (HC-PBFs) exhibit extremely low environmental sensitivity [2], which makes them promising for use in fiber optic gyroscopes (FOGs). It has been demonstrated that the nonlinear Kerr-induced phase drifts, thermally induced Shupe error, and Faraday effect are substantially reduced in a hollow-core photonic bandgap fiber-optic gyroscope (HC-PBFOG) compared to those of the conventional FOG [3]–[7].

The connection between HC-PBF coil and integrated-optic circuit (IOC) is a key technology for the improvement in HC-PBFOG performance, which requires low back-reflection, low loss, and high reliability at the splicing point [8]–[10]. The first HC-PBFOG proposed by Stanford University has employed butt coupling between HC-PBF coil and pigtails of the IOC. The structure is very simple, and has a coupling loss of ∼2.7 dB at the butt coupling junction [4]. However, it has low reliability, and the coupling performance is prone to change over the full temperature range. Xu *et al.* [8] have used fusion splicing between HC-PBF coil and IOC pigtails in HC-PBFOG, in which both HC-PBF coil and pigtails of the IOC were angle-cleaved at ∼8° to suppress back-reflection. However, the method has led to problems such as a large splicing loss because of collapse of air holes in HC-PBF in the vicinity of the splicing joint and extremely low splicing strength due to the holey structure of the HC-PBF. Moreover, the angle cleaving of the HC-PBF has increased the complexity. Jung *et al.* [11] have proposed a butt coupling method to interconnect SMF to

The associate editor coordinating the review of this manuscript and approving it for publication was Md. Selim Habib.

HCF-PBF using micro-optic collimator. The method achieves high-quality coupling performance, but the structure is too complicated and large for the FOG (the length is ∼7 cm). Therefore neither the butt coupling nor the fusion splicing between the HC-PBF coil and IOC pigtails in HC-PBFOG are perfect coupling methods. They cannot satisfy the practical requirements of HC-PBFOG. It is actually the connection between the HC-PBF and the traditional fiber whether by butt coupling or fusion splicing, which would cause a variety of non-reciprocity errors and they can be suppressed by direct coupling between fiber coil and IOC [10], [12], [13]. Therefore, the direct coupling of HC-PBF and IOC is a key technology that must be broken through for high-performance HC-PBFOGs [14]. A direct coupling method of HC-PBF with IOC has been proposed [15], in which there is no air gap between HC-PBF and IOC, but it involves precise angle-cleaving operation of the HC-PBF end-face and precise polishing of the adapter attachment face that must be angled at the same angle as the end-face of HC-PBF. Moreover, the complicated process includes experimental determination of the optimum angle, fabrication of the angle, and reinstalling of the HC-PBF and adapter.

In this study, we propose a simple and optimized method for the coupling between HC-PBF and IOC based on those previous works. The end-face of HC-PBF only needs to be flat-cleaved with a general fiber cleaver without other operations such as special angle-cleaving or polishing. The optimal coupling angle is determined and experimentally verified to overcome the effect of the air gap between the flat-cleaved HC-PBF and the angle-cleaved IOC. The samples can achieve maximum loss and back-reflection of ∼3.2 dB and ∼−43 dB, respectively. This coupling method provides a foundation for the direct coupling between HC-PBF coil and IOC in the future.

II. THEORY AND SIMULATIONS

The schematic of coupling between HC-PBF and IOC is illustrated in Fig. 1. The IOC is angle-cleaved to $\theta_c = \sim 10°$ as traditional IOC to suppress back-reflection at the end-face [10]. Considering that the end-face of HC-PBF cannot be polished or processed with complex operations as the conventional fiber owing to the existence of air holes, the HC-PBF is only flat-cleaved with a general fiber cleaver, which is easily implemented in practice. The flat-cleaved HC-PBF is coupled with the angle-cleaved IOC at a specific coupling angle (θ) which is defined as the angle between the HC-PBF center axis and normal of the IOC end-face. As a result, as shown in Fig. 1, an air gap (Δ) must exist between the end-face of IOC and HC-PBF, which includes $\Delta_1 = R \cdot \cot\theta$ and additional gap Δ_2, where R is radius of the HC-PBF cladding. This air gap causes the light to diverge before entering the hollow core of HC-PBF from IOC or entering IOC from HC-PBF, thus decreasing coupling efficiency. However, the coupling angle (θ) can be optimized to reduce the effect of the air gap and obtain as low loss as possible for the coupling point.

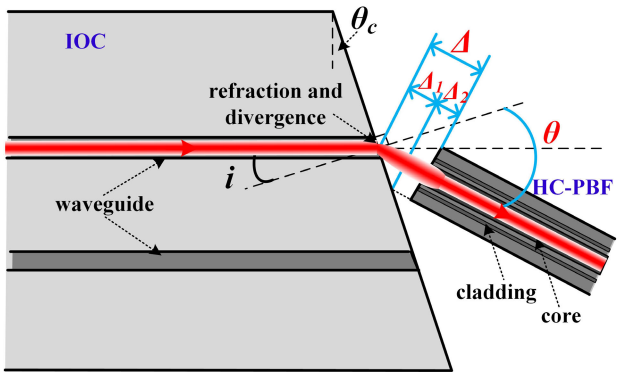

FIGURE 1. Schematic of the coupling of HC-PBF with IOC (The schematic only shows the light coupled to HC-PBF from IOC). The flat-cleaved HC-PBF is coupled with the angle-cleaved IOC at a specific coupling angle (θ) and air gap (Δ). The beam refracts at the end-face of IOC and quickly expands upon traveling through the air gap (Δ).

A. BACK-REFLECTION SUPPRESSION

As shown in Fig. 1, the back-reflection in the coupling between HC-PBF and IOC originates from the end-face of HC-PBF and IOC. The back-reflection (∼−80 dB) originated from the end-face of HC-PBF can be theoretically neglected [16], which is a considerable advantage and unique characteristic of the HC-PBF. The back-reflection originated from IOC end-face is suppressed by traditional cleaving and polishing at $\theta_c = \sim 10°$ [10]. Therefore, the back-reflection is not a problem in the schematic.

B. COUPLING LOSS REDUCTION

The coupling loss includes three parts, mode mismatch, Fresnel reflection, and misalignment losses [17]. The mode field characteristics of HC-PBF and IOC are measured by a camera-based beam profiler system. The seven-cell HC-PBF (Fig. 2(a)) used in this study has a circle mode (Φ ∼9 μm at 1550 nm), as illustrated in Fig. 2(b). The mode of the IOC is an ellipse (∼8.5 μm × ∼6.5 μm at 1550 nm), as shown in Fig. 2(c). The mode mismatch loss calculated by overlap integral is only ∼0.45 dB [18], and thus it is not the main part. The Fresnel reflection loss calculated by reflectivity is only ∼0.71 dB and thus can also be neglected [10].

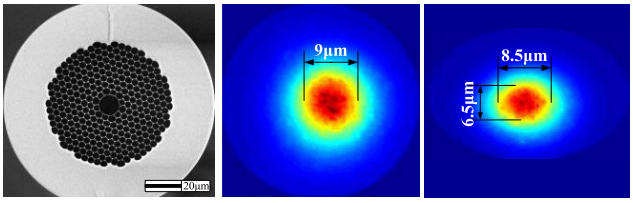

FIGURE 2. (a) Scanning electron microscopy image of the cross section of the HC-PBF. Test results for the mode fields of the (b) HC-PBF and (c) IOC.

The misalignment loss originates as the end-face is not perfectly aligned when the HC-PBF is coupled to the IOC,

which is the most important source of the coupling loss. The angle-cleaved IOC can effectively suppress the back-reflection, but causes beam refraction at the end-face of the IOC. HC-PBF is inherently a multi-mode fiber. When it is coupled with IOC, mode mismatch and misalignment will not only produce coupling loss, but also excite unwanted higher-order modes in the HC-PBF. In order to suppress the excitation of higher-order modes and improve the coupling efficiency between the fundamental modes of the HC-PBF and IOC, the mode mismatch and the coupling misalignment should be minimized. The IOC has a mode field profile similar to the HC-PBF (Fig. 2(b) and (c)), and the calculated mode mismatch loss is only ∼0.45 dB. The structure and mode field characteristics of the IOC used in a FOG make it unsuitable for using mode field adapter (such as graded-index fiber [19] and micro-lens [11]) to achieve mode field matching with HC-PBF. For the coupling between IOC and HC-PBF, adding a mode field adapter will increase the coupling loss (the connection between the IOC and the mode field adapter will cause Fresnel reflection and misalignment losses). Therefore, the most effective measure to reduce coupling loss and suppress higher-order mode excitation is to minimize the misalignment.

To reduce the misalignment loss while suppressing excitation of higher-order modes, the beam should be incident ideally along the center axis of the HC-PBF. The transmission direction of the refracted light can be calculated based on the Snell's law to determine the coupling angle (θ). However, the air gap (Δ) increases the coupling loss because the optical mode emerging from the IOC or the HC-PBF quickly expands upon traveling through the air gap, as illustrated in Fig. 1. A larger air gap Δ implies a larger mode field divergence. Thus, the end-face of HC-PBF should be as close to the end-face of IOC as possible, i.e., Δ_2 is better to be 0. Moreover, the coupling angle θ should be optimized to guarantee both reduction of the air gap (Δ_1) and successful acceptance of the light for HC-PBF or IOC.

To obtain the maximum coupling efficiency, it is necessary to comprehensively consider the alignment deviation and mode field divergence to determine the optimal coupling angle θ. According to the schematic in Fig. 1, a three-dimensional model of the coupling between IOC and HC-PBF is given in Fig. 3. The beam propagation method is used to simulate the light transmission, and the coupling efficiency for different coupling angles θ and different air gaps Δ_2 are calculated. As shown in Fig. 4(a), the maximum efficiency of coupling from IOC to HC-PBF reaches ∼87.26% when the coupling angle θ is ∼15° and the air gap Δ_2 is 0 μm, which corresponds to a loss of ∼0.6 dB; the maximum efficiency of coupling from HC-PBF to IOC reaches ∼58.73% when the coupling angle θ is ∼20° and the air gap Δ_2 is 0 μm, which corresponds to a loss of ∼2.3 dB. Considering that both coupling directions simultaneously exist for a FOG, the total bidirectional coupling efficiency has the maximum value (∼47.32%) when the coupling angle (θ)

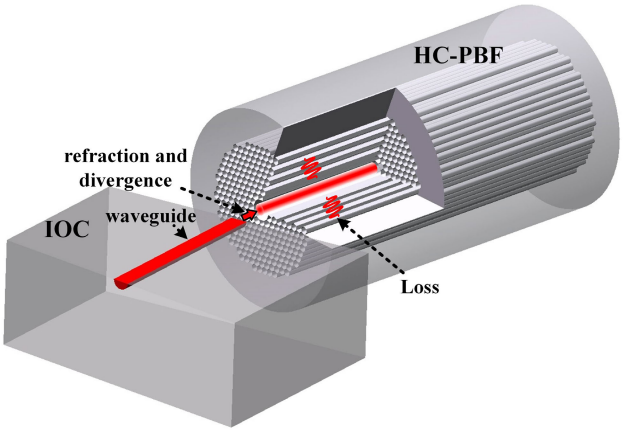

FIGURE 3. Model of the coupling of the flat-cleaved HC-PBF with the angle-cleaved IOC (The model only shows the light coupled to HC-PBF from IOC).

and air gap (Δ_2) are ∼18.7° and 0 μm, respectively, which corresponds to a loss of ∼3.2 dB, as shown by the red curve in Fig. 4(a). In practice, it is difficult for the fiber end-face to be just attached to the IOC and make the air gap Δ_2 equal zero. The simulation results in Fig. 4(b) reveal that the bidirectional coupling efficiency almost linearly decreases as the increase of Δ_2 with a slope of ∼−0.07 dB/μm, which is very small and thus reduces the requirement for longitudinal alignment accuracy.

In fact, HC-PBF is a multi-mode fiber, so the transitional process of modes in the HC-PBF and IOC during the coupling is simulated with beam propagation method. As shown in Fig. 5(a), when the light transmitted in the HC-PBF is coupled to the IOC, a large number of higher-order modes are immediately excited, but these higher-order modes are attenuated rapidly when they transmit in the IOC, and ultimately only the fundamental mode remains. Correspondingly, when the light transmitted in the IOC is coupled to the HC-PBF, higher-order modes are also excited in the HC-PBF, and most of them are attenuated and lost during transmission, as shown in Fig. 5(b). Simulation results show that reducing the misalignment can effectively suppress the excitation of higher-order modes in the HC-PBF, and coupling of the light from HC-PBF to IOC can better reveal the coupling between the fundamental modes.

III. EXPERIMENT AND RESULTS

An experiment setup is established to determine the coupling angle θ and verify the simulation results, as shown in Fig. 6. The amplified spontaneous emission (ASE) broad-band light is coupled into the IOC pigtail. A 10°-polished IOC is placed on a three-axis displacement stage (X, Y, Z) to precisely adjust the additional gap Δ_2. A seven-cell HC-PBF (Fig. 2(a)) having a flat end-face obtained with an ordinary cleaver is placed on a two-axis rotation stage (pitch and yaw) to precisely adjust the coupling angle θ. The length of the HC-PBF is ∼2 m.

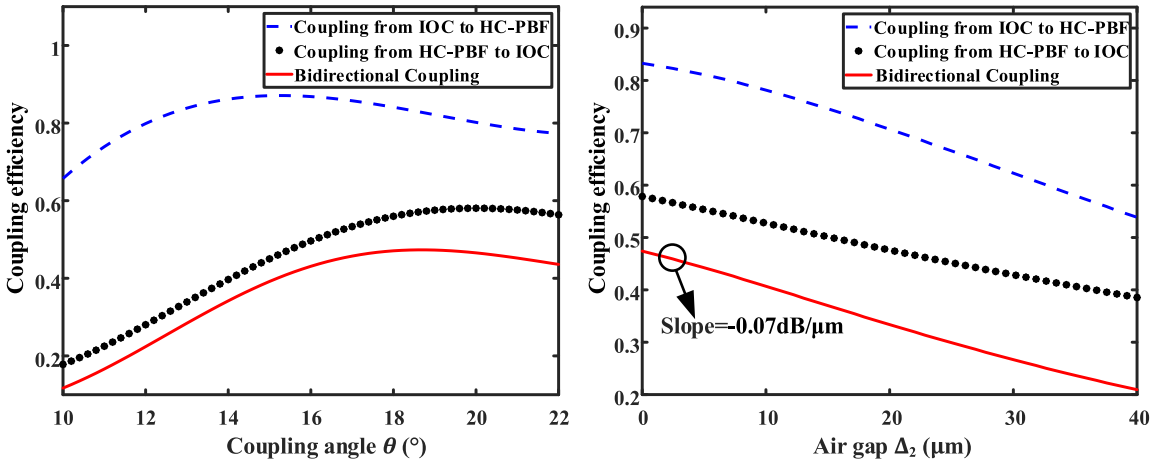

(a) Coupling efficiency at different coupling angles θ and air gap Δ_2 of 0

(b) Coupling efficiency at different air gaps Δ_2 and coupling angle θ of 18.7°.

FIGURE 4. Simulation of the coupling efficiency. The maximum total bidirectional efficiency of coupling from HC-PBF to IOC and IOC to HC-PBF reaches ∼47.32% when the coupling angle θ is ∼18.7° and the air gap Δ_2 is 0 μm (red curve).

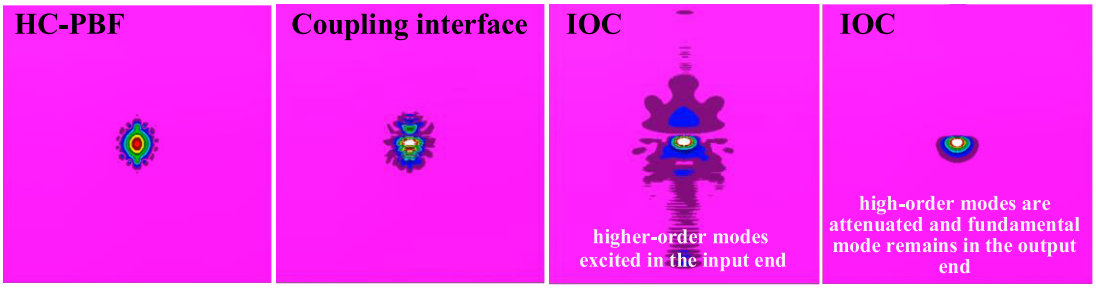

(a) Coupling from HC-PBF to IOC

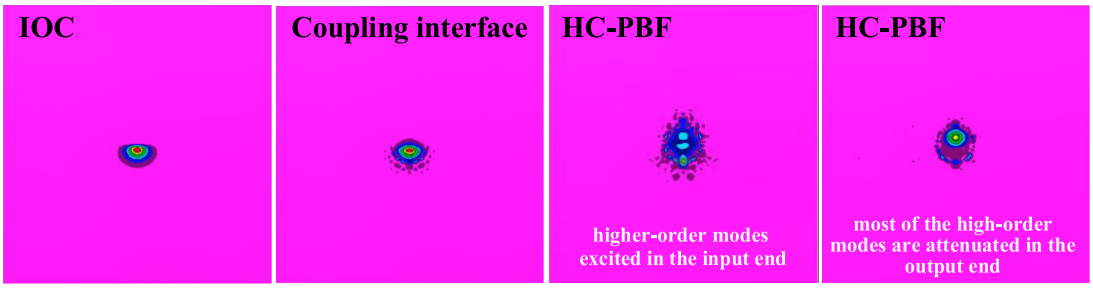

(b) Coupling from IOC to HC-PBF

FIGURE 5. The transitional process of modes during coupling of HC-PBF with IOC.

A. VERIFICATION AND DETERMINATION OF COUPLING ANGLE

The misalignment between HC-PBF and IOC does not only increase the coupling loss, but also cause the higher-order modes to be excited in the HC-PBF. Therefore, the coupling angle should be optimized to minimize the misalignment and improve the coupling efficiency of fundamental modes between HC-PBF and IOC. First, we investigate the influence of the coupling angle θ on the efficiency of coupling from IOC to HC-PBF. The mode of the IOC output is only the fundamental mode. The flat end-face of the HC-PBF is coupled to the circuit at different coupling angles by adjusting the two-axis rotation stage. The HC-PBF should be as close as possible to the IOC to obtain an air gap Δ_2 close to 0 during the coupling by adjusting the three-axis displacement stage. Most of the higher-order modes excited in the HC-PBF are attenuated and lost after they transmit through the ∼2-m fiber, but a few higher-order modes remain. The output optical power of the HC-PBF including the fundamental mode and remaining higher-order modes is monitored in real

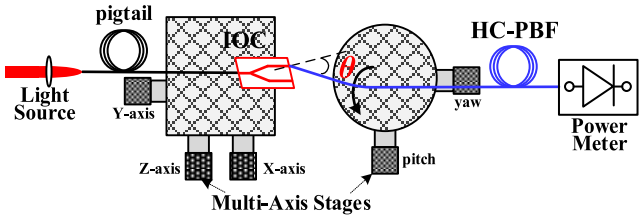

FIGURE 6. Experiment setup for the determination of the coupling angle θ (The setup only shows the light coupled to HC-PBF from IOC).

time by power meter (AV6334) to determine the coupling efficiency. Therefore, the coupling loss for this direction reflects the coupling efficiency between fundamental mode of the IOC and modes (fundamental mode and some higher-order modes) of the HC-PBF. The experimental results are shown by the blue curve in Fig. 7, which reveal that the coupling efficiency is maximum when the coupling angle is ∼18°. Second, we investigate the optimal coupling angle for the opposite coupling direction, i.e., when the light is coupled from HC-PBF to IOC. The experimental results are presented by the black curve in Fig. 7, which shows that the coupling efficiency has the maximum value when the coupling angle is ∼20°. The distribution of the output mode field of the HC-PBF is measured by a camera-based beam profiler system, which proves that the output of HC-PBF is basically only the fundamental mode, as shown in Fig. 2(b). The output mode of the IOC is also only the fundamental mode, so the coupling for this direction reveals the coupling efficiency of fundamental modes between HC-PBF with IOC. Consequently, we can use the coupling efficiency when the light is coupled from HC-PBF to IOC to characterize the loss performance of the method.

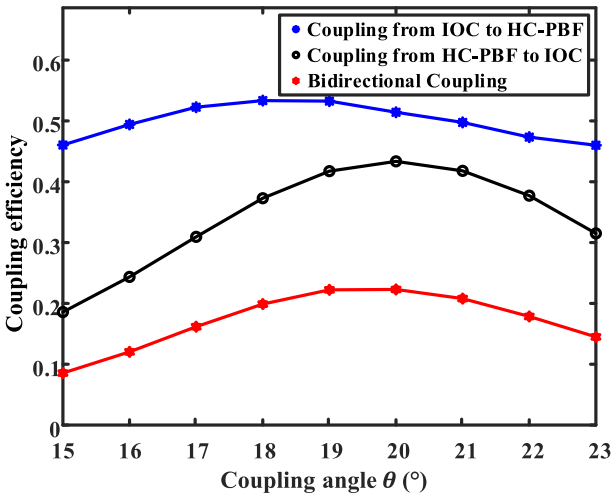

FIGURE 7. Experimentally determined coupling efficiency at different coupling angles θ. The bidirectional coupling efficiency (red curve) has the maximum value of 22.29% when the coupling angle is ∼19°.

As shown by the red curve in Fig. 7, the total coupling efficiency for both directions has the maximum value of 22.29% which corresponds to a loss of ∼6.5 dB when the coupling angle is ∼19°. The experimental results agree well with the simulation results. In addition, the small slope of the red curve around 19° indicates a larger misalignment tolerance for the coupling angle around 19°. The calculated 1 dB penalty misalignment tolerance is ∼ ±2° for the coupling angle around 19°. Consequently, the angular requirements for the attachment face of the fiber adapter and its mounting can be significantly reduced, which is very important in practice.

B. PERFORMANCE OF THE PROTOTYPES AND DISCUSSION

Based on the schematic and analysis mentioned above, the flat-cleaved HC-PBF is fixed with a special adapter which is bonded to the 10°-cleaved IOC and makes the coupling angle equal ∼19°. The material of the adapter used to fix the coupling point is lithium-niobate, which is the same as the material of the IOC and important for the stable performance over full temperature range. Ten prototypes are fabricated, as shown in Fig. 8. The maximum coupling loss from IOC to HC-PBF is ∼2.95 dB, and the loss from HC-PBF to IOC is ∼3.32 dB, as shown in Fig. 9(a). As mentioned above, the coupling loss from HC-PBF to IOC can better characterize the coupling efficiency between fundamental modes of the HC-PBF and the IOC. The coupling between HC-PBF and IOC has non-reciprocal loss, mainly because higher-order modes are excited in the HC-PBF when the light is coupled from IOC to HC-PBF [20], [21]. The main reason for the excitation of higher-order modes in HC-PBF may be that the mode expands upon traveling through the air gap (Δ) which increases the mode mismatch between IOC and HC-PBF. In fact, the flat-cleaving method brings simplicity and convenience as compared to [15], but the induced air-gap between HC-PBF and IOC causes mode field divergence and increases the mode mismatch. As a result, higher-order modes will be excited in the fiber due to mode field mismatch, and the output modal content of the HC-PBF obtained by the optical coherence domain polarimeter shows that the output modes contain a higher-order mode (LP_{11}), and its power is ∼5% of the power of fundamental mode, so the coupling loss between the fundamental modes when the light is coupled from IOC

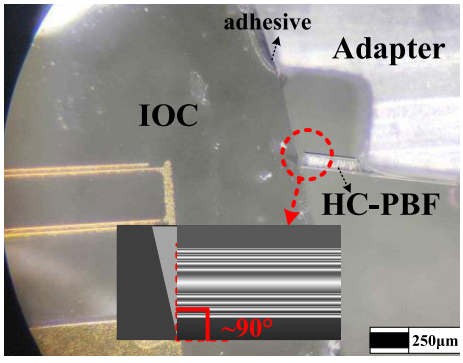

FIGURE 8. Prototype of the coupling of flat-cleaved HC-PBF with angle-cleaved IOC.

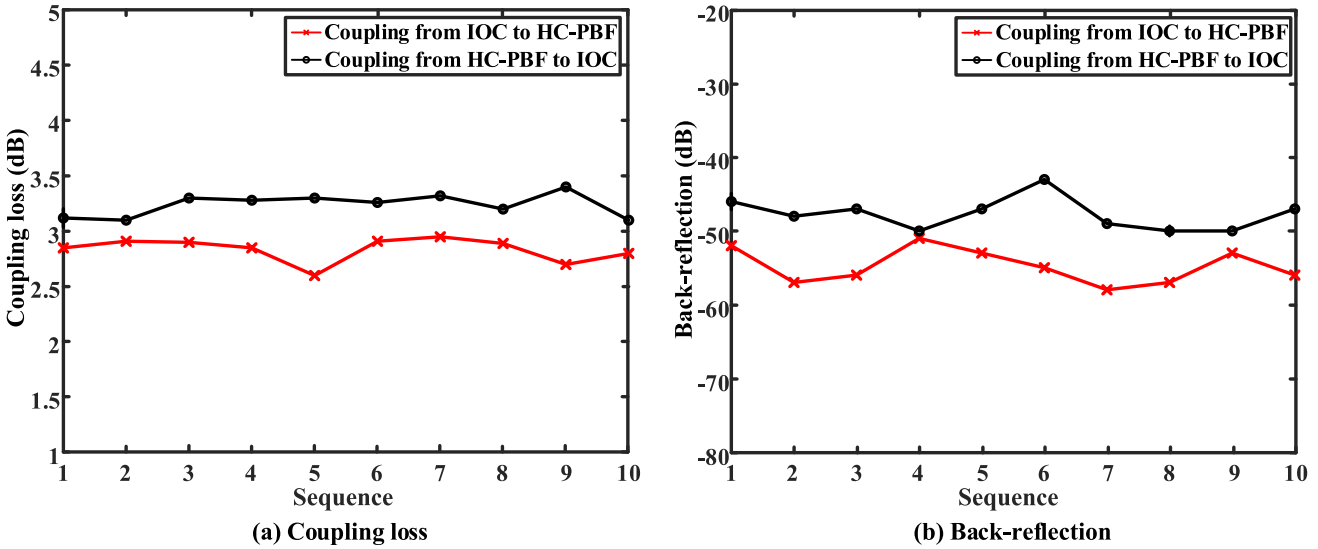

FIGURE 9. Test results for the prototypes.

to HC-PBF is ∼3.16 dB after the higher-order modes are considered, which is close to the loss from HC-PBF to IOC (∼3.32 dB). However, these higher-order modes will be attenuated and lost after transmitting hundreds, even thousands of meters of HC-PBF in the fiber coil (the attenuation of LP_{11} mode is calculated in COMSOL to be ∼90 dB/km at 1550 nm), thus having little effect on the performance of the FOG. The maximum back-reflection for the direction from IOC to HC-PBF is ∼−51 dB, which is slightly larger than the back-reflection performance (∼60 dB) for traditional fiber and IOC [10], possibly as the other side of the IOC end-face is not SiO_2 but air, and residual reflection on the IOC end-face is stronger. The maximum back-reflection for the direction from HC-PBF to IOC is ∼−43 dB. In fact, this experimental result is a little far from the theoretical expectation (∼−80 dB) [16], which may be caused by stray light caused by divergent light's scattering on the imperfect end-face of IOC, but it is sufficient for the application in a FOG [10].

IV. CONCLUSION

In summary, we proposed a simple and practical method for low-loss low-back-reflection coupling of HC-PBF with IOC. The end-face of the HC-PBF only needed to be flat-cleaved with a general fiber cleaver without other complex operations such as polishing or special angle-cleaving. The optimal coupling angle of ∼18.7° was determined and experimentally verified to overcome the effect of the air gap between flat-cleaved HC-PBF and 10°-cleaved IOC. What is more, 1 dB penalty misalignment tolerance is ∼ ±2° for the coupling angle around the optimal coupling angle, which reduced the requirements for coupling accuracy and the difficulty of alignment. The experimental results demonstrated that the coupling loss between the fundamental modes was better than ∼3.2 dB, and back-reflection of HC-PBF with IOC was better than ∼−43 dB.

This method can be used for other types of hollow-core fibers, such as polarization-maintaining hollow-core fibers, where it is required to only replace the two-axis rotation stage (pitch and yaw) to a three-axis stage (pitch, yaw, and roll), so that the alignment of the polarization axis can be achieved. Therefore, this study provides a foundation for the direct coupling of HC-PBF coil to IOC in HC-PBFOG, which will be our aim in the future.

REFERENCES

[1] H. C. Lefèvre, "Potpourri of comments about the fiber optic gyro for its 40th anniversary, and how fascinating it was and it still is!" in *Proc. SPIE*, Baltimore, MD, USA, vol. 9852, 2016, Art. no. 985203.
[2] R. Slavik, E. N. Fokoua, M. N. Petrovich, N. V. Wheeler, T. Bradley, F. Poletti, and D. J. Richardson, "Ultralow thermal sensitivity of phase and propagation delay in hollow-core fibres," in *Proc. Eur. Conf. Opt. Commun. (ECOC)*, Gothenburg, Sweden, Sep. 2017, pp. 1–3.
[3] H. K. Kim, V. Dangui, M. Digonnet, and G. Kino, "Fiber-optic gyroscope using an air-core photonic-bandgap fiber," in *Proc. SPIE*, vol. 5855, 2005, pp. 198–201.
[4] H. Kyun Kim, M. J. F. Digonnet, and G. S. Kino, "Air-core photonic-bandgap fiber-optic gyroscope," *J. Lightw. Technol.*, vol. 24, no. 8, pp. 3169–3174, Aug. 2006.
[5] S. Blin, H. K. Kim, M. J. F. Digonnet, and G. S. Kino, "Reduced thermal sensitivity of a fiber-optic gyroscope using an air-core photonic-bandgap fiber," *J. Lightw. Technol.*, vol. 25, no. 3, pp. 861–865, Mar. 2007.
[6] S. W. Lloyd, V. Dangui, M. J. F. Digonnet, S. H. Fan, and G. S. Kino, "Measurement of reduced backscattering noise in laser-driven fiber optic gyroscopes," *Opt. Lett.*, vol. 35, no. 2, pp. 121–123, Jan. 2010.
[7] S. Lloyd, S. H. Fan, and M. J. F. Digonnet, "Improving fiber optic gyroscope performance using a laser and photonic-bandgap fiber," in *Proc. SPIE*, Beijing, China, vol. 8421, 2012, pp. 84210B-1–84210B-4.
[8] X. Xu, N. Song, Z. Zhang, and J. Jin, "Backward secondary-wave coherence errors in photonic bandgap fiber optic gyroscopes," *Sensors*, vol. 16, pp. 851-1–851-7, Jun. 2016.
[9] X. Xu, Z. Zhang, Z. Zhang, J. Jin, and N. Song, "Method for measurement of fusion-splicing-induced reflection in a photonic bandgap fiber-optical gyro," *Chin. Opt. Lett.*, vol. 13, no. 3, pp. 030601-1–030601-4, Mar. 2015.
[10] H. C. Lefevre, *The Fiber-Optic Gyroscope*, 2nd ed. Norwood, MA, USA: Artech House, 2014.

[11] Y. Jung, H. Kim, Y. Chen, T. D. Bradley, I. A. Davidson, J. R. Hayes, G. Jasion, H. Sakr, S. Rikimi, F. Poletti, and D. J. Richardson, "Compact micro-optic based components for hollow core fibers," *Opt. Express*, vol. 28, no. 2, pp. 1518–1525, Jan. 2020.
[12] B. E. Kincaid, "Coupling of polarization-maintaining optical fibers to Ti:$LiNbO_3$ waveguides with angled interfaces," *Opt. Lett.*, vol. 13, no. 5, pp. 425–427, May 1988.
[13] N. Mekada, M. Seino, Y. Kubota, and H. Nakajima, "Practical method of waveguide-to-fiber connection: Direct preparation of waveguide endface by cutting machine and reinforcement using ruby beads," *Appl. Opt.*, vol. 29, no. 34, pp. 5096–5102, Dec. 1990.
[14] T. A. Morris and M. J. F. Digonnet, "Broadened-laser-driven polarization-maintaining hollow-core fiber optic gyroscope," *J. Lightw. Technol.*, vol. 38, no. 4, pp. 905–911, Feb. 15, 2020.
[15] K. Steven, "Hollow core fiber pigtail system and method," U.S. Patent 0 347 986, Dec. 6, 2018.
[16] X. Xu, M. Yan, C. Wu, N. Song, and C. Zhang, "Experimental investigation of backreflection at air-core photonic bandgap fiber terminations," *Opt. Laser Technol.*, vol. 92, pp. 198–201, Jul. 2017.
[17] J. A. Hammond, "Scale-factor variations due to wavelength-dependent optical losses in fiber optic gyros," in *Proc. SPIE*, Denver, Co, USA, vol. 2837, 1996, pp. 239–248.
[18] R. Alferness, V. Ramaswamy, S. Korotky, M. Divino, and L. Buhl, "Efficient single-mode fiber to titanium diffused lithium niobate waveguide coupling for $\lambda = 1.32\ \mu$m," *IEEE J. Quantum Electron.*, vol. 18, no. 10, pp. 1807–1813, Oct. 1982.
[19] M. Komanec, D. Suslov, S. Zvanovec, Y. Chen, T. Bradley, S. R. Sandoghchi, E. R. N. Fokoua, G. T. Jasion, M. N. Petrovich, F. Poletti, D. J. Richardson, and R. Slavik, "Low-loss and low-back-reflection hollow-core to standard fiber interconnection," *IEEE Photon. Technol. Lett.*, vol. 31, no. 10, pp. 723–726, May 15, 2019.
[20] R. Thapa, K. Knabe, K. L. Corwin, and B. R. Washburn, "Arc fusion splicing of hollow-core photonic bandgap fibers for gas-filled fiber cells," *Opt. Express*, vol. 14, no. 21, pp. 9576–9583, Oct. 2006.
[21] K. Z. Aghaie, M. J. F. Digonnet, and S. H. Fan, "Optimization of the splice loss between photonic-bandgap fibers and conventional single-mode fibers," *Opt. Lett.*, vol. 35, no. 12, pp. 1938–1940, Jun. 2010.

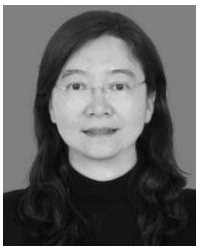

NINGFANG SONG received the B.E. degree from Harbin Engineering University, Harbin, China, in 1989, and the M.E. and Ph.D. degrees from Beihang University, Beijing, China, in 1993 and 2004, respectively. She is currently a Professor with the School of Instrument Science and Opto-Electronics Engineering, Beihang University. Her current research interests include fiber-optic gyroscopes and inertial navigation systems.

CHENG HE received the B.E. degree from Beihang University, Beijing, China, in 2018, where he is currently pursuing the M.E. degree. His current research interests include hollow-core photonic bandgap fibers.

XIAOBIN XU received the B.E. degree from the Hefei University of Technology, Hefei, China, in 2003, and the Ph.D. degree from Beihang University, Beijing, China, in 2010. He is currently an Associate Professor with the School of Instrument Science and Opto-Electronics Engineering, Beihang University. His current research interests include microstructure fibers and fiber sensors.

JIAQI LIU was born in Shanxi, China, in 1993. She received the bachelor's degree from the School of Automation, Harbin Engineering University, Harbin, China, in 2016. She is currently pursuing the Ph.D. degree with the School of Instrumentation Science and Opto-Electronics Engineering, Beihang University, Beijing, China. Her main research interests include integrated optics and optical sensors.

FUYU GAO received the B.E. degree from Beihang University, Beijing, China, in 2014, where he is currently pursuing the Ph.D. degree. His current research interests include photonic-crystal fibers.

YUNHAO ZHU received the B.E. degree from Beihang University, Beijing, China, in 2017, where he is currently pursuing the Ph.D. degree. His current research interests include photonic-crystal fibers and fiber optic gyroscope.